

## Pathological matrix stiffness promotes cardiac fibroblast differentiation through the POU2F1 signaling pathway

Mingzhe Li<sup>1</sup>, Jimin Wu<sup>1</sup>, Guomin Hu<sup>1</sup>, Yao Song<sup>1</sup>, Jing Shen<sup>1</sup>, Junzhou Xin<sup>1</sup>, Zijian Li<sup>1</sup>, Wei Liu<sup>2</sup>, Erdan Dong<sup>1,3</sup>, Ming Xu<sup>1</sup>, Youyi Zhang<sup>1\*</sup> & Han Xiao<sup>1\*</sup>

<sup>1</sup>Department of Cardiology and Institute of Vascular Medicine, Peking University Third Hospital; NHC Key Laboratory of Cardiovascular Molecular Biology and Regulatory Peptides; Key Laboratory of Molecular Cardiovascular Science, Ministry of Education; Beijing Key Laboratory of Cardiovascular Receptors Research, Beijing 100191, China;

<sup>2</sup>Division of Cardiovascular Sciences, Faculty of Biology Medicine and Health, University of Manchester, Manchester M13 9PT, UK;

<sup>3</sup>Institute of Cardiovascular Sciences, Health Science Center, Peking University, Beijing 100191, China

Received December 16, 2019; accepted May 21, 2020; published online June 29, 2020

Cardiac fibroblast (CF) differentiation into myofibroblasts is a crucial cause of cardiac fibrosis, which increases in the extracellular matrix (ECM) stiffness. The increased stiffness further promotes CF differentiation and fibrosis. However, the molecular mechanism is still unclear. We used bioinformatics analysis to find new candidates that regulate the genes involved in stiffness-induced CF differentiation, and found that there were binding sites for the POU-domain transcription factor, POU2F1 (also known as Oct-1), in the promoters of 50 differentially expressed genes (DEGs) in CFs on the stiffer substrate. Immunofluorescent staining and Western blotting revealed that pathological stiffness upregulated POU2F1 expression and increased CF differentiation on polyacrylamide hydrogel substrates and in mouse myocardial infarction tissue. A chromatin immunoprecipitation assay showed that POU2F1 bound to the promoters of fibrosis repressors IL1R2, CD69, and TGIF2. The expression of these fibrosis repressors was inhibited on pathological substrate stiffness. Knockdown of POU2F1 upregulated these repressors and attenuated CF differentiation on pathological substrate stiffness (35 kPa). Whereas, overexpression of POU2F1 downregulated these repressors and enhanced CF differentiation. In conclusion, pathological stiffness upregulates the transcription factor POU2F1 to promote CF differentiation by inhibiting fibrosis repressors. Our work elucidated the crosstalk between CF differentiation and the ECM and provided a potential target for cardiac fibrosis treatment.

**fibroblast differentiation, matrix stiffness, POU2F1, cardiac fibrosis, transcription factor**

**Citation:** Li, M., Wu, J., Hu, G., Song, Y., Shen, J., Xin, J., Li, Z., Liu, W., Dong, E., Xu, M., et al. (2021). Pathological matrix stiffness promotes cardiac fibroblast differentiation through the POU2F1 signaling pathway. *Sci China Life Sci* 64, 242–254. <https://doi.org/10.1007/s11427-019-1747-y>

### INTRODUCTION

Cardiac fibrosis is a typical pathological process that occurs in various heart diseases, including myocardial infarction (MI), aortic stenosis, and cardiomyopathy, and it ultimately leads to the progression of heart failure (Li et al., 2018). Cardiac fibrosis is characterized by excessive accumulation

of extracellular matrix (ECM) proteins in the cardiac interstitium (Feng et al., 2018; Kong et al., 2014; Segura et al., 2014). ECM proteins are mainly synthesized and secreted from myofibroblasts (Gyongyosi et al., 2017; Herum et al., 2017; Hinz et al., 2007; van Putten et al., 2016), and myofibroblasts are primarily differentiated from cardiac fibroblasts (CFs), one of the most abundant cell types in the heart (Souders et al., 2009). The accumulation of ECM proteins during cardiac fibrosis increases in the stiffness of cardiac tissue. However, the increased stiffness can further promote

\*Corresponding authors (Youyi Zhang, email: [zhangyy@bjmu.edu.cn](mailto:zhangyy@bjmu.edu.cn); Han Xiao, email: [xiaohan@bjmu.edu.cn](mailto:xiaohan@bjmu.edu.cn))

the process of cardiac fibrosis (Herum et al., 2017; Zhao et al., 2014), and ECM stiffness has been reported to induce CF differentiation (Elson et al., 2019; Engler et al., 2006; Zhao et al., 2014). Our group previously found that CFs displayed a nonmonotonic elasticity variation with an increase in substrate stiffness (Shi et al., 2011). However, the mechanism by which matrix stiffness promotes CF differentiation has not been fully elucidated. It is important to clarify the mechanism, as gaining this knowledge may lead to significant progress in blocking cardiac fibrosis and the progression of heart failure.

Several distinct pathways have been studied for their role in the mechanosensing of ECM stiffness in CFs. On the plasma membrane, integrin, toll-like receptors, and syndecans are reported to sense ECM stiffness (Li and Chaikof, 2002; Scheibner et al., 2006; Taylor et al., 2004; Zaidel-Bar et al., 2007). In the cytoplasm, the TGF $\beta$  (Huelsz-Prince et al., 2013; Jenkins, 2008; Rahaman et al., 2014; Robertson et al., 2015; Song et al., 2014; Yang et al., 2016; Zilberberg et al., 2012), ROCK (Driesen et al., 2014; Ni et al., 2013; Xie et al., 2014) and Hippo signaling pathways (Aragona et al., 2013; Codelia et al., 2014; Dupont et al., 2011) respond to stiffness and induce fibrosis. In addition, HSP, IL1 $\alpha$ , NF $\kappa$ B, and HMGB1, which are involved in the MAPK signaling pathway and the AGE-RAGE signaling pathway, contribute to the stiffness-induced release of ECM proteins (Strand et al., 2015; Tian et al., 2007; Turner, 2014; Vabulas et al., 2001). In the nucleus, the LINC (linker of nucleoskeleton and cytoskeleton) complex, including NESPRINs, SUN and LAMINs, was reported to be involved in mechanotransduction (Herum et al., 2017). In addition, transcription factors in the nucleus were also regulated by stiffness (Wang et al., 2009). Nonetheless, the crosstalk and the shared regulatory mechanism of these distinct signaling pathways are still incompletely understood. It is unknown whether there is a core factor in the regulation of these multiple pathways involved in ECM stiffness-induced CF differentiation.

Here, to investigate the core factor regulating substrate stiffness-induced CF differentiation, we used published RNA-seq data to identify the differentially expressed genes (DEGs) in CFs cultured on substrates with different levels of stiffness. Bioinformatics analysis was used to predict the transcription factors of these genes and to identify a transcription factor that can regulate the largest number of DEGs. The analysis results suggested that POU domain class 2 transcription factor 1 (POU2F1, also known as Oct-1) is a crucial candidate whose binding sites were found in 50 DEGs. POU2F1 expression was found to change in CFs cultured on pathological substrates with different levels of stiffness and was additionally found to have a role in the regulation of CF differentiation. This research will improve our understanding of the role of substrate stiffness in CF differentiation and will provide a potential target for the

treatment of cardiac fibrosis.

## RESULTS

### Transcriptome change in CFs under different substrate stiffness

To identify candidates that regulate multiple downstream genes responding to substrate stiffness, we conducted bioinformatics analysis. The global transcriptional profiles of CFs cultured on substrates with different stiffnesses were obtained from the NCBI's Gene Expression Omnibus database (GSE113277) (Yu et al., 2018). Compared with gene expression in CFs on the softer substrate (8 kPa), 303 DEGs (filtering criteria  $P < 0.05$ , fold-change  $> 2.0$ ) were identified in CFs on the stiffer substrate (64 kPa) (Table S1 in Supporting Information). These genes included 272 downregulated and 31 upregulated genes (Figure 1A and B). Gene Ontology (GO) enrichment was listed based on the annotation of three categories: molecular function, cellular component, and biological process (Figure 1C–E; Table S2 in Supporting Information). The levels of 111 DEGs responding to the stimulus changed when the cells were cultured with the stiffer substrate (GO: 0050896). Sixty-one DEGs were involved in cell differentiation (GO: 0030154). The DEGs (172 genes) are mainly involved in the intracellular systems (GO: 0044424). The analysis emphasized that the DEGs with the ion binding (GO: 0043167) ability played important roles in response to substrate stiffness. Ninety-one of the 303 genes have been previously reported to be associated with fibrosis in the PubMed database (Table S3 in Supporting Information). STRING analysis (Szklarczyk et al., 2011) also revealed that the functional links of 67 of these 91 DEGs were associated with responding to stimulus (GO: 0050896), and 34 of these 91 DEGs participated in responding to stress (GO: 0006950) (Figure 1F; Table S3 in Supporting Information).

The position weight matrix algorithm in TRANSFAC was used to predict the potential transcription factors of the 91 DEGs that have been reported to be involved in fibrosis. The top 10 transcription factors that were predicted to bind to the greatest number of DEGs are listed in Figure 1G and Table S4 (in Supporting Information). Nkx2-5 was predicted to bind to the most DEGs (54 DEGs). A previous study reported that Nkx2-5 regulates CF differentiation and fibrosis (Dritsoula et al., 2018). The putative binding site for the transcription factor POU2F1 was predicted in the promoter regions of 50 DEGs (Figure 1G). Among the 50 DEGs, five were upregulated and 45 were downregulated. In these 50 DEGs, there were 41 DEGs related to the “physiological response to stimulus (GO: 0050896)”, 20 DEGs related to the “response to stress (GO: 0006950)”, and 11 DEGs related to the “regulation of cell differentiation (GO: 0045595)”

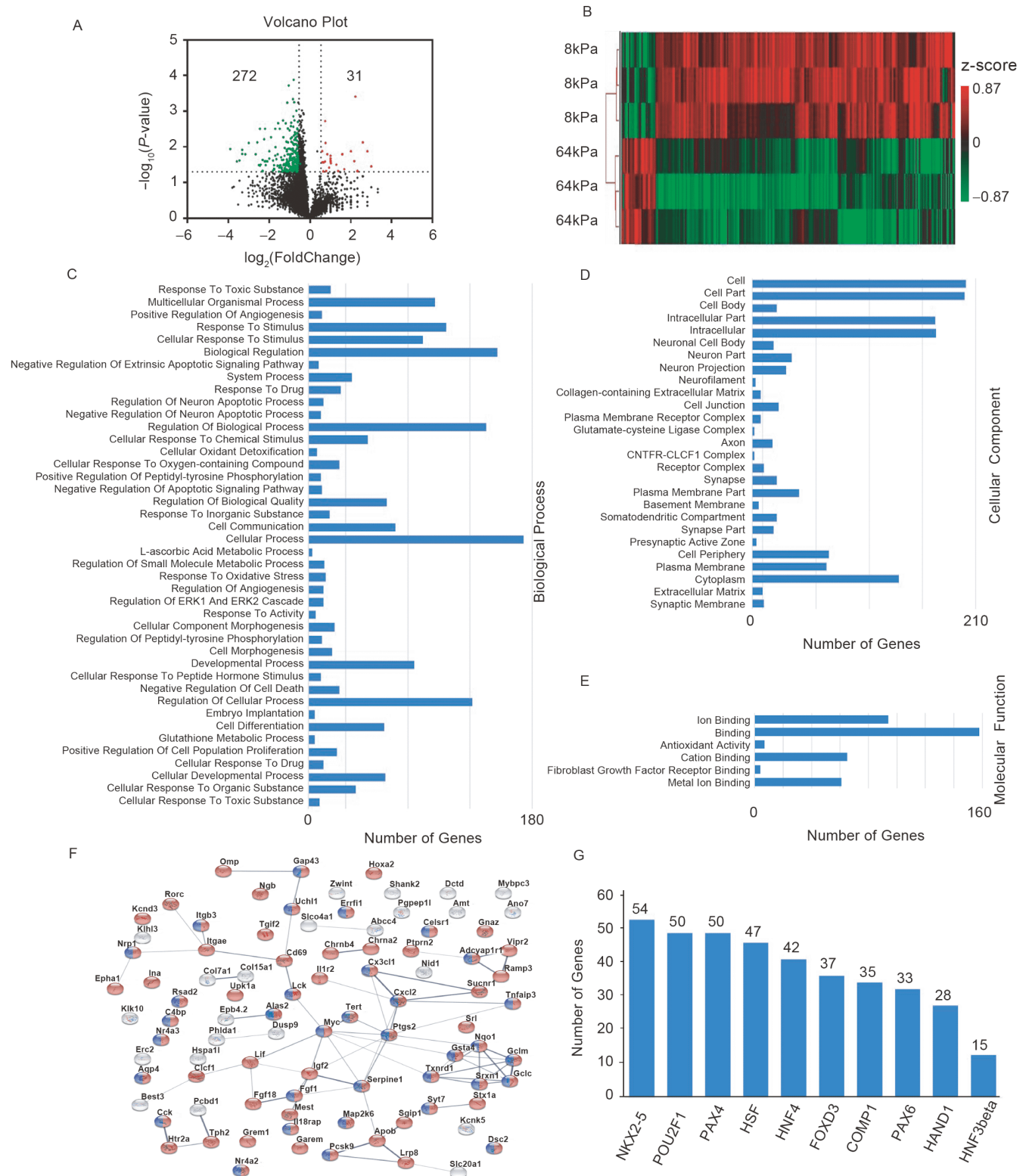


**Figure 1** Transcriptome analysis of CFs grown on substrates with different stiffnesses. **A**, Volcano analysis of differentially expressed genes (DEGs) between CFs grown on softer and stiffer substrates. The red dots and green dots represent upregulated and downregulated DEGs, respectively, with statistical significance. **B**, Expression profiles of mRNA in CFs grown on softer and stiffer substrates. **C**, Biological process (GO) annotation of transcripts. **D**, Cellular component (GO) annotation of transcripts. **E**, Molecular function (GO) annotation of transcripts. **F**, STRING analysis reveals protein interaction networks in fibrosis-related genes in the stiffer/softer comparison group. Red: involved in response to stimulus (GO: 0050896); blue: involved in response to stress (GO: 0006950). **G**, The top 10 transcription factors predicted to bind to the greatest number of DEGs by TRANSFAC. The number shows the amount of DEGs with predicted binding sites of the indicative transcription factor.

(Table S5 in Supporting Information). This information indicates that POU2F1 plays a crucial role in sensing the stiffness and inducing CF differentiation.

### The protein level of POU2F1 was upregulated in response to substrates with pathological stiffness

POU2F1 is a new potential target identified in the present study, and its role in stiffness-induced cardiac fibrosis has not been reported. Before we studied the expression of POU2F1 in response to different substrate stiffness, we first cultured CFs on polyacrylamide hydrogels with different stiffnesses and assessed the morphological change in CFs by characterizing the F-actin distribution; these assessments were performed to ensure that this *in vitro* substrate stiffness system was effective. The stiffness of 7.5 kPa is similar to the stiffness of the infarct region (Herum et al., 2017); 13 kPa is comparable to that of the healthy myocardium (Hinz, 2009); both 19.5 kPa and 35 kPa mimic the stiffness in fibrotic myocardium and in scar tissue of the infarct region (Herum et al., 2017). Consistent with previous reports, CFs exhibited a round and elongated form on softer hydrogels, and they had a greater extent of cell spreading and were star-shaped when cultured on stiffer hydrogels (Figure S1 in Supporting Information).

We examined the distribution and expression of POU2F1 in response to different substrate stiffnesses. POU2F1 was predominantly located in the nucleus (Figure 2A). The expression pattern of POU2F1 was the lowest in CFs cultured on a physiological stiffness (13 kPa) substrate. Compared with physiological stiffness (13 kPa), the softer and stiffer pathological stiffness resulted in a higher protein expression level of POU2F1 in CFs on the substrate (Figure 2A and B). The POU2F1 mRNA level also increased in CFs cultured on the softer or stiffer substrate (Figure 2C), suggesting that the expression of POU2F1 was regulated by different substrate stiffness at the transcriptional level. To gain insight into the *in vivo* relevance, we detected the protein level of POU2F1 in different phases of the MI model. The protein level of POU2F1 in the infarct region was significantly upregulated within 1 day (3 kPa), 4 days (stiffer than physiological tissue), and 7 days (close to 30 kPa) after MI. As a reference, there was no apparent change in the protein level of POU2F1 in the remote region (the stiffness was similar to that in healthy tissue, Figure 2D). Collectively, these results indicated that pathological stiffness upregulated POU2F1 expression both *in vitro* and *in vivo*.

The differentiation of CF into myofibroblasts is characterized by an increase in the expression of fibronectin and  $\alpha$ -smooth actin ( $\alpha$ SMA) (Hinz et al., 2007; Pankov and Yamada, 2002). Immunofluorescent staining showed that the protein levels of fibronectin and  $\alpha$ SMA in CFs were the lowest on 13 kPa (physiological stiffness) polyacrylamide

hydrogels. Both softer and stiffer substrates induced an increase in the protein levels of fibronectin and  $\alpha$ SMA (Figure 2E). Consistently, Western blotting revealed that fibronectin and  $\alpha$ SMA were upregulated on the 19.5 kPa substrate and further increased on the 7.5 kPa and 35 kPa substrates, compared with the 13 kPa substrate (Figure 2F). These results indicated that fibroblast differentiation was induced by pathological stiffness.

### POU2F1 bound to the promoter of the predicted downstream genes

To validate whether POU2F1 can bind to the promoter of the predicted target genes, we selected three candidate genes from the TRANSFAC bioinformatics analysis, IL1R2, CD69, TGIF2. They were chosen as representatives because they not only have the putative POU2F1-binding site, but they are also reported to play similar roles in inhibiting cardiac fibrosis. The putative POU2F1-binding sites were predicted in the promoter region of these three genes (Figure 3A–C). The chromatin immunoprecipitation (ChIP) assay revealed that the fraction containing the IL1R2, CD69 and TGIF2 promoters was significantly higher than that containing the control regions, suggesting that POU2F1 bound to the three gene promoters (Figure 3D–F). Compared with CFs cultured on a physiological substrate (13 kPa), the expression pattern of all three genes was downregulated in CFs cultured on a pathological substrate (35 kPa) (Figure 3G–I). These results indicated that pathological stiffness regulated the gene expression of IL1R2, CD69 and TGIF2 and may be associated with POU2F1 binding to their promoters.

### POU2F1 suppressed the expression of IL1R2, CD69 and TGIF2 in CFs on a substrate with pathological stiffness

To determine the role of POU2F1 in the expression of the candidate genes involved in stiffness-induced CF differentiation, we knocked down POU2F1 and determined the expression of IL1R2, CD69 and TGIF2 on pathological stiffness (35 kPa) substrate by qRT-PCR and Western blotting. The mRNA and protein levels of POU2F1 were significantly reduced in the POU2F1 knockdown group (Figure 4A and B). The expression levels of IL1R2, CD69 and TGIF2 significantly increased following POU2F1 knockdown on the 35 kPa substrate (Figure 4C–H). We also investigated whether POU2F1 overexpression decreases IL1R2, CD69 and TGIF2 expression. Mouse POU2F1 expression cassette in the pAdeasy adenoviral vector was constructed (Figure 4J). The protein level of POU2F1 was significantly increased in the ad-POU2F1 infected group (Figure 4I). As expected, the protein levels of IL1R2, CD69 and TGIF2 were decreased in POU2F1 adenovirus-infected CFs (Figure 4K–M). Thus, POU2F1 inhibited the expression



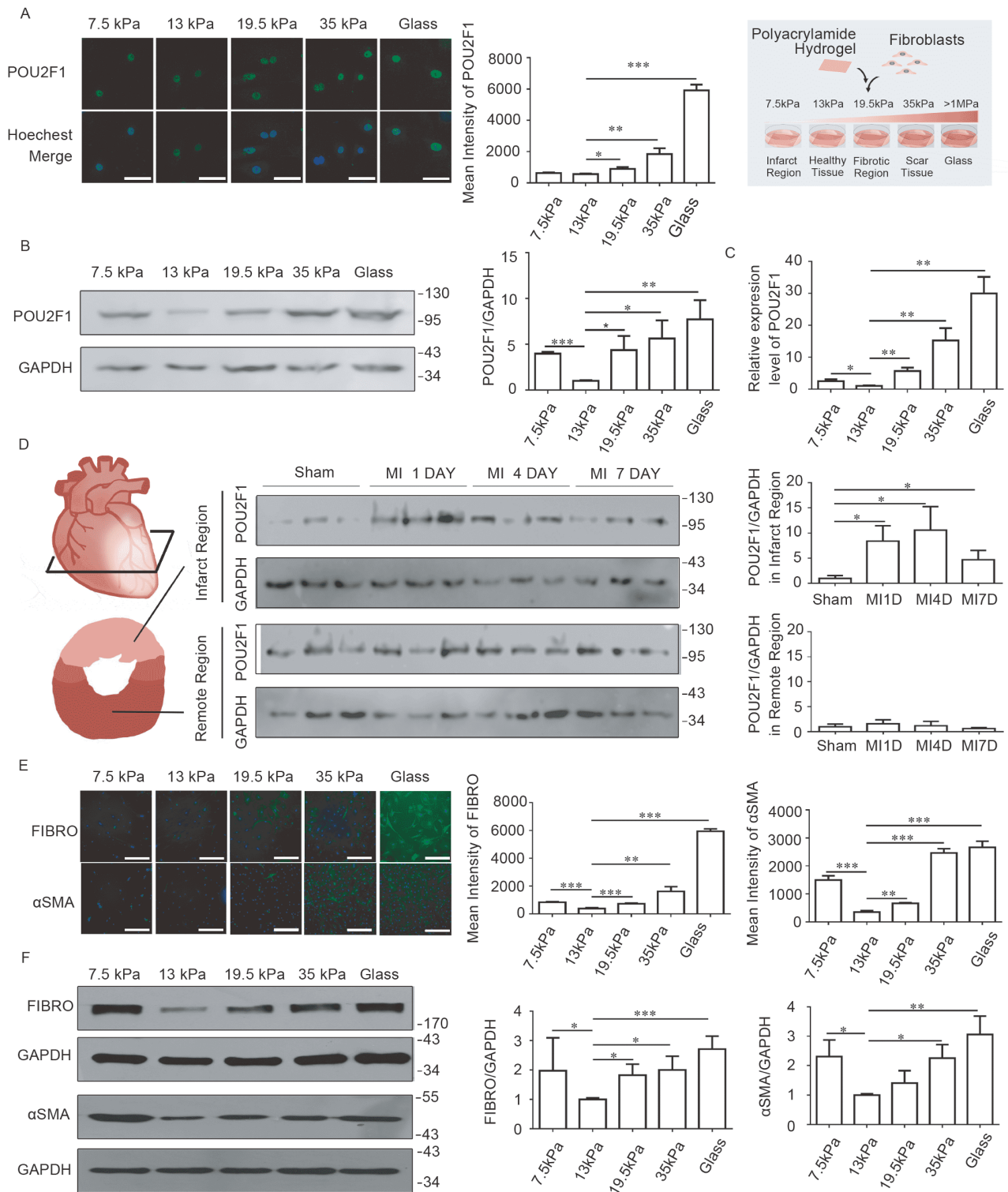


**Figure 2** Pathological stiffness upregulated POU2F1 expression both *in vitro* and *in vivo*. **A**, Representative immunofluorescence images and quantification of POU2F1 (green) and nuclei (blue) in CFs by high-content screening imaging; scale bar, 50  $\mu$ m;  $n=5$ . CFs were cultured on the substrate with different stiffnesses. Right panel illustrates the relationship of hydrogel stiffness and heart tissue. **B**, Western blotting and quantification of POU2F1 on hydrogel substrates with a stiffness gradient,  $n=5$ . **C**, Quantitative real-time PCR of POU2F1 on hydrogel substrates with a stiffness gradient,  $n=5$ . **D**, Western blotting and quantification of POU2F1 in the infarct region and remote region within 1, 4, and 7 days after MI,  $n=3$ . **E**, Quantification of the myofibroblast marker fibronectin (green) and  $\alpha$ SMA (green) by high-content screening imaging, nuclei (blue); scale bar, 100  $\mu$ m;  $n=5$ . **F**, Western blotting and quantification of the myofibroblast marker fibronectin and  $\alpha$ SMA on hydrogel substrates with a stiffness gradient,  $n=5$ . Data are shown as the mean $\pm$ SD. \* $P<0.05$ , \*\* $P<0.01$ , \*\*\* $P<0.001$ , using one-way ANOVA with Tukey's post hoc test or with Games-Howell post-hoc test, or Kruskal-Wallis ANOVA combined with post hoc Dunn's multiple comparison test.

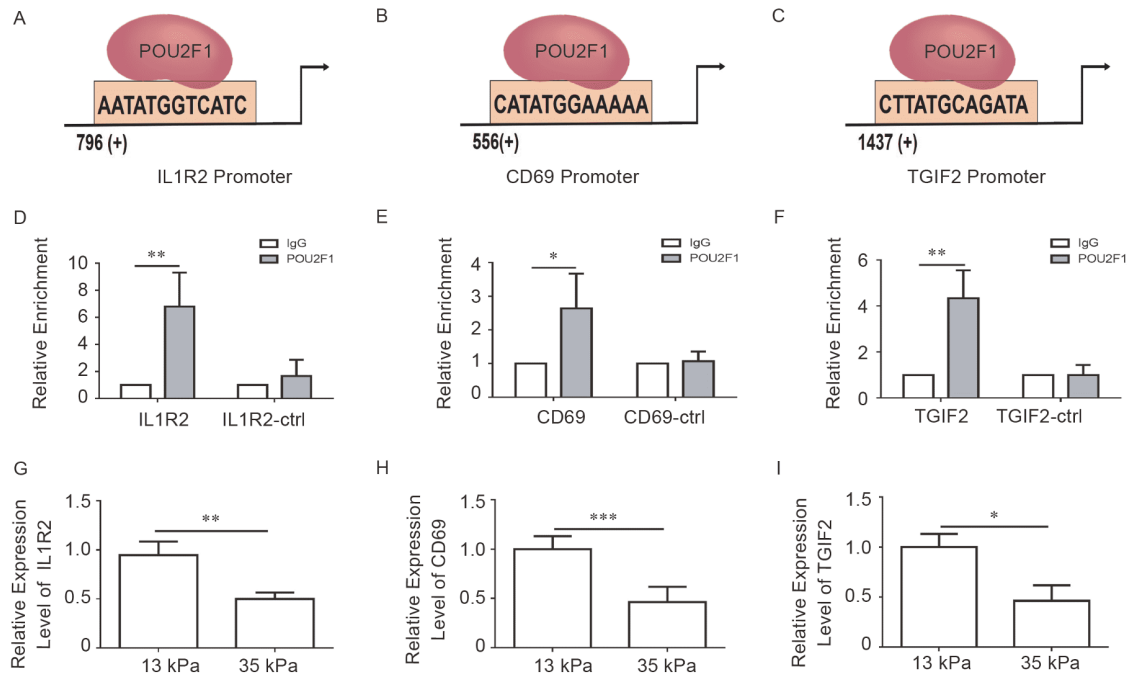


**Figure 3** (Color online) POU2F1 binds to the promoters of IL1R2, CD69 and TGIF2. A–C, Schematic of the interaction of POU2F1 with the IL1R2 (A), CD69 (B) and TGIF2 (C). The number shows the position of the predict binding site in the promoter + strand. The pink box indicates the putative motif that can be bound by POU2F1. D–F, ChIP assay using the anti-POU2F1 antibody confirms the binding of POU2F1 to the IL1R2 (D), CD69 (E) and TGIF2 (F) promoters in CFs,  $n=5$ . G–I, Relative expression of IL1R2 (G), CD69 (H) and TGIF2 (I) in CFs on substrates with stiffnesses of 13 and 35 kPa,  $n=5$ . Data are shown as the mean $\pm$ SD. \* $P<0.05$ , \*\* $P<0.01$ , \*\*\* $P<0.001$ , using Student's  $t$ -test, Welch's  $t$ -test or the Mann-Whitney  $U$ -test.

of the three fibrosis repressors in CFs on pathological stiffness substrate.

### Substrate stiffness modulated CF differentiation through POU2F1

To verify the function of POU2F1 in pathological stiffness-induced CF differentiation, the protein level of myofibroblast markers in POU2F1-knockdown CFs was detected on pathological stiffness (35 kPa) hydrogels by immunofluorescent staining and Western blotting. The green fluorescence of fibronectin and  $\alpha$ SMA became weaker in POU2F1-knockdown CFs (Figure 5A and B). Western blotting also showed that the protein levels of fibronectin and  $\alpha$ SMA significantly decreased after knockdown of POU2F1 (Figure 5C). In contrast, the protein levels of fibronectin and  $\alpha$ SMA increased in POU2F1 overexpressed CFs (Figure 5D). These results indicated that POU2F1 promoted pathological stiffness-induced fibroblast differentiation.

## DISCUSSION

The present study first found that the transcription factor POU2F1 plays a crucial role in the crosstalk between ECM stiffness and CF differentiation. POU2F1 was upregulated by pathological substrate stiffness and promoted CF differ-

entiation by inhibiting fibrotic repressors, including IL1R2, CD69 and TGIF2. Our findings have provided a new core link between ECM stiffness and CF differentiation and suggested POU2F1 as a potential therapeutic target for cardiac fibrosis (Figure 6).

POU2F1 is the only widely expressed member of the POU factor family (Hinz et al., 2007; Pankov and Yamada, 2002). About half of the members in the family display a substantial affinity for an 8 bp DNA site termed the octamer motif, and hence POU2F1 is also known as Oct-1. POU2F1 associates with different cofactors to mediate either transcriptional activation, repression, or gene poising (Shakya et al., 2011; Zhang et al., 1999). The mRNA and protein levels of POU2F1 significantly increase in various cancers (Shakya et al., 2011; Zhang et al., 1999). Initially, POU2F1 was described to target genes associated with proliferation and immune modulation (Vazquez-Arreguin and Tantin, 2016). Recent studies identified that its targets are also associated with oxidative and cytotoxic stress resistance, metabolic regulation, stem cell function and other unexpected processes (Borlak and Thum, 2002; Boulon et al., 2002; Cairns et al., 2011; Kang et al., 2009; Kang et al., 2013; Maddox et al., 2012; Magne et al., 2003). However, the role of POU2F1 in the heart is not fully understood, especially in cardiac fibrosis.

We analyzed the transcriptome data of fibroblasts on different stiffness (8 and 64 kPa) as a clue for investigating the

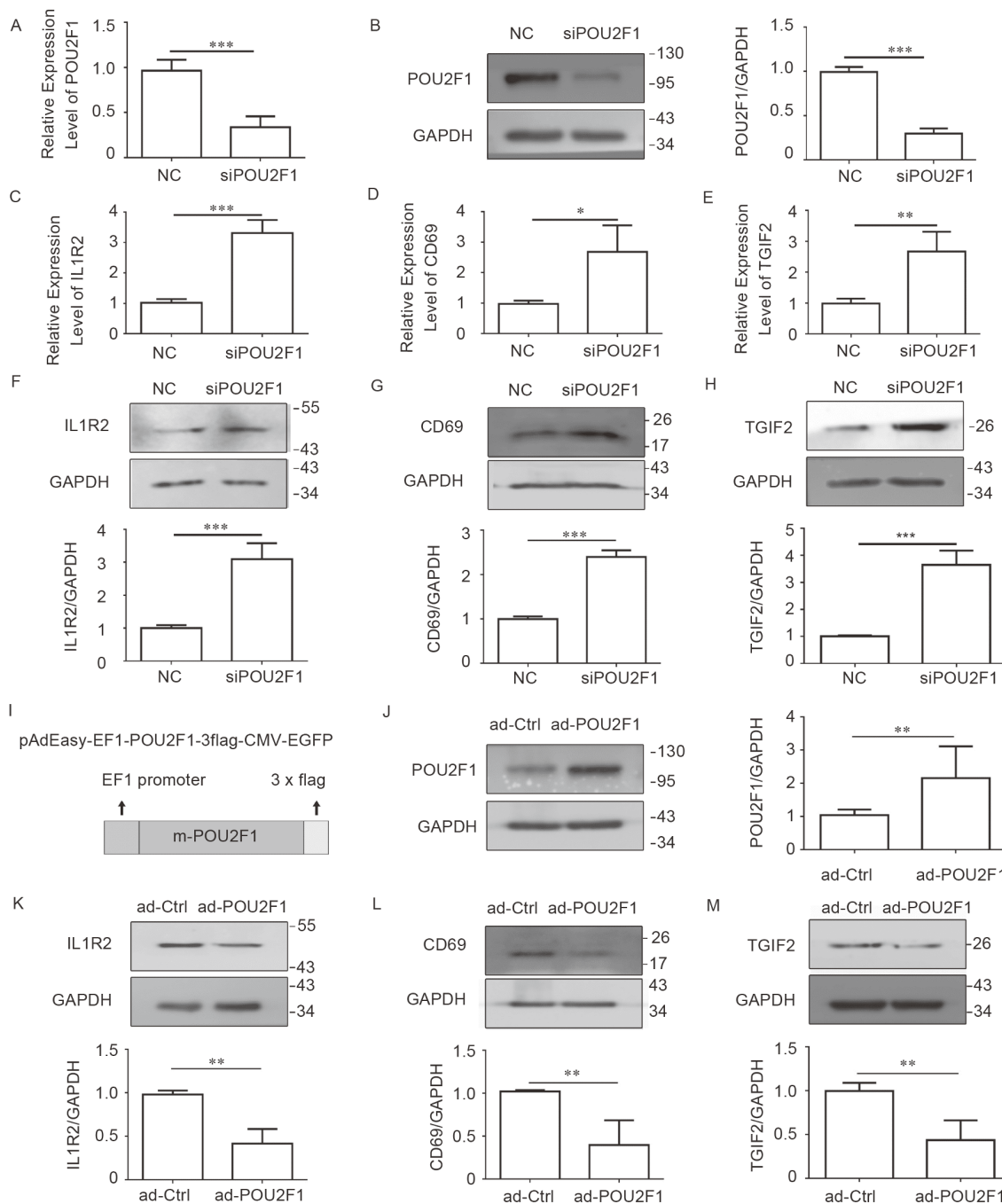


**Figure 4** POU2F1 negatively regulates IL1R2, CD69 and TGIF2 expression. A and B, Verification of the knockdown efficiency of POU2F1 siRNA. Quantitative real-time PCR (A) and Western blotting (B) experiments of POU2F1 were conducted after separately transfecting siRNAs into CFs for one and three days,  $n=5$ . C–E, Relative expression of IL1R2 (C), CD69 (D) and TGIF2 (E) in POU2F1-knockdown CFs compared with that in negative control (NC) cells on a substrate with a stiffness of 35 kPa,  $n=5$ . F–H, Western blotting and quantification of IL1R2 (F), CD69 (G) and TGIF2 (H) in POU2F1-knockdown CFs compared with that in NC cells on a substrate with a stiffness of 35 kPa,  $n=5$ . I, The structure schematic of the adenovirus engineered to overexpress mouse POU2F1 (m-POU2F1). J–M, Western blotting and quantification of POU2F1 (J), IL1R2 (K), CD69 (L) and TGIF2 (M) in ad-POU2F1 infected CFs compared with that in ad-Ctrl infected cells,  $n=5$ . Data are shown as the mean $\pm$ SD. \* $P<0.05$ , \*\* $P<0.01$ , \*\*\* $P<0.001$ , using Student's  $t$ -test, Welch's  $t$ -test or the Mann-Whitney  $U$ -test.

underlying mechanism of stiffness-induced fibrosis. It indicated that POU2F1 is the possible key regulatory factor. The stiffness range of normal heart under physiological conditions is estimated as 10–20 kPa, and 20–100 kPa for the

fibrotic myocardium (Berry et al., 2006; Conrad et al., 1995; Engler et al., 2008; Torres et al., 2018; Wu et al., 2000). The physiological cardiac stiffness (13 kPa) in the present study was chosen according to the above-mentioned knowledge

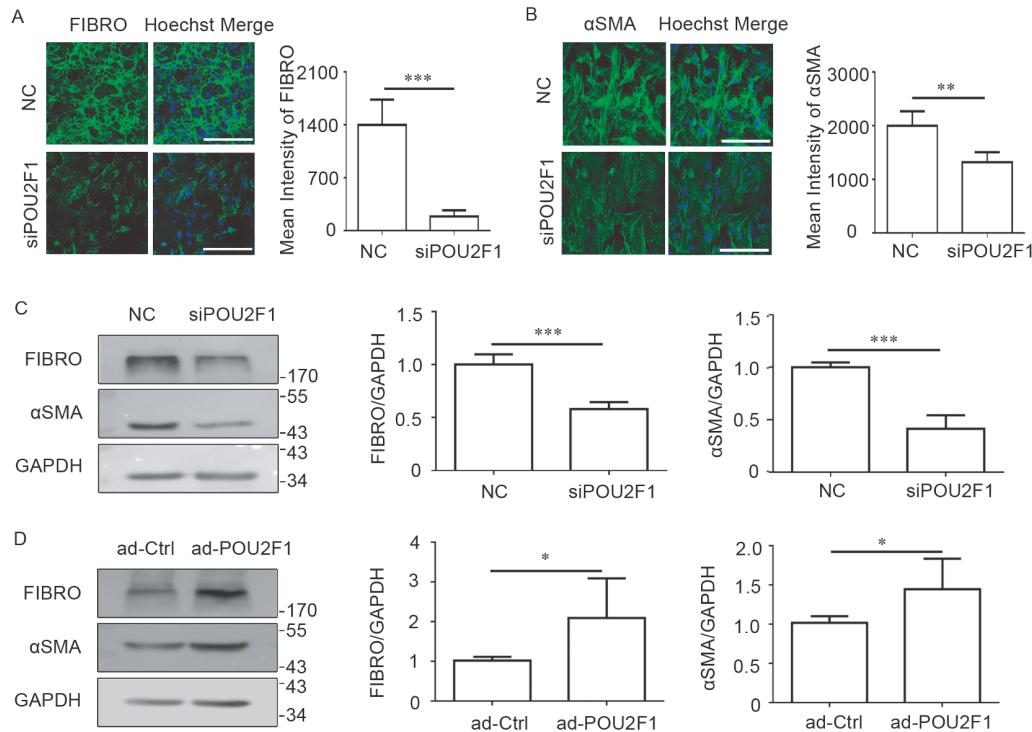


**Figure 5** Roles of POU2F1 in fibroblast differentiation. A and B, CFs were transfected with POU2F1 siRNA or negative control (NC) and cultured on a substrate with a stiffness of 35 kPa. Immunofluorescence and quantification of the myofibroblast marker fibronectin (A) and  $\alpha$ SMA (B) in CF cells. Nuclei were labeled with Hoechst (blue); scale bar, 100  $\mu$ m;  $n=5$ . C, Western blotting and quantification of fibronectin and  $\alpha$ SMA in POU2F1-knockdown CFs,  $n=5$ . D, Western blotting and quantification of fibronectin and  $\alpha$ SMA in CFs infected with ad-Ctrl or ad-POU2F1,  $n=5$ . Data are shown as the mean $\pm$ SD. \*,  $P<0.05$ ; \*\*,  $P<0.01$ ; \*\*\*,  $P<0.001$ , using Student's *t*-test or Welch's *t*-test.

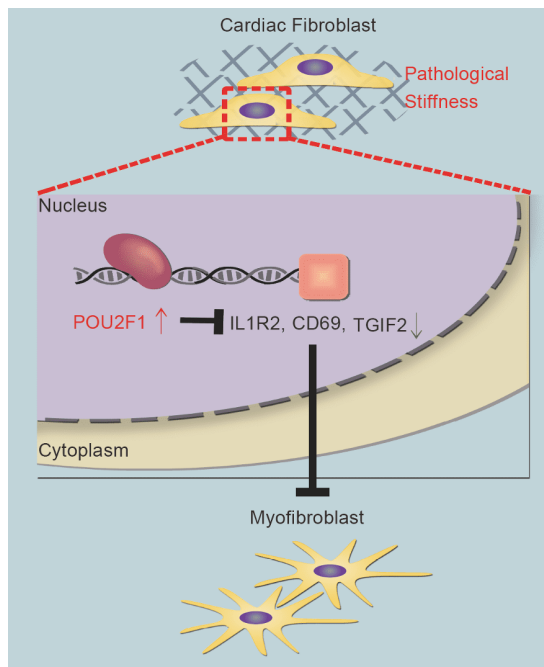


**Figure 6** Schematic summary of the role of POU2F1 in pathological stiffness-induced CF differentiation. During the pathological process, the abnormal alteration in stiffness of substrates, both stiffer or softer, upregulates POU2F1. POU2F1 inhibits the transcription of fibrosis repressors, IL1R2, CD69 and TGIF2, which results in the differentiation of CFs to myofibroblasts.

and our group's previous publication (Shi et al., 2011). According to these studies, we selected the substrate stiffness (7.5, 13, 19.5 and 35 kPa) to investigate the effect and mechanism of stiffness on CF differentiation in the present study.

Following MI, the infarct region showed softer stiffness initially (within 1 day), and the stiffness continuously increased to higher stiffness than normal after the acute phase. In the present study, we found that both softer and stiffer substrate stiffness could promote POU2F1 expression and CF differentiation. The softer stiffness-induced fibrosis, which occurs in the early phase following myocardial infarction, is considered protective against heart rupture (Talmán and Ruskoaho, 2016). Hence, POU2F1 may be important for cardiac repair during the acute phase by promoting softer stiffness-induced CF differentiation. However, in the later phase, the cardiac tissue gradually becomes stiffer than physiological condition. The fibrosis enhanced by stiffer stiffness is deleterious and can promote pathological cardiac remodeling. Exaggerated fibrosis leads to impairments in cardiac function and ultimately heart failure (Talmán and Ruskoaho, 2016). During this process, cardiac fibrosis results in an increase in matrix stiffness, which will further aggravate fibrosis (Herum et al., 2017). Thus, we focused on the stiffer stiffness-induced CF differentiation



and chose 35 kPa to study the mechanism how stiffer substrate regulates CF differentiation. The present study suggests that POU2F1 is a newly identified crucial factor in this vicious cycle, which will finally result in heart failure. In addition, the heart failure marker beta-myosin heavy chain is reported as the downstream target gene of POU2F1 (Allen et al., 2005; Lakich et al., 1998). Therefore, POU2F1 is critical to the regulation of cardiac fibrosis and may be a potential target for the treatment of cardiac fibrosis and heart failure.

Both the mRNA and protein levels of POU2F1 were up-regulated during stiffness-induced CF activation. Several studies identified elevated levels of POU2F1 mRNA and protein in cancer compared with normal tissues (Vazquez-Arreguin and Tantin, 2016). But the upstream regulative mechanism of POU2F1 expression has not been extensively investigated. It is reported that POU2F1 is modified by ubiquitylation, but the ubiquitin ligase(s) and deubiquitinases are still unknown (Kang et al., 2013). Focal adhesion kinase (FAK) acts as a mechanosensor by modulating cell proliferation in response to changes in tissue compliance (Thomas et al., 2019). Matrix stiffness regulates cell differentiation through FAK signaling pathway (Thomas et al., 2019). FAK promotes protein degradation through ubiquitination, leading to cell growth and proliferation (Zhou et al., 2019). It is possible that FAK may be involved in stiffness-induced POU2F1 expression. Overall, how pathological stiffness upregulates POU2F1 needs further study in the future.

IL1R2, CD69 and TGIF2 were identified as the target genes of POU2F1. They are known as fibrotic suppressors. IL1R2 is a decoy receptor that inhibits IL-1 signal and fibrosis (Shimizu et al., 2015). It interacts with IL1R1 to inhibit the activity of its ligands (IL1A and IL1B) (Borthwick, 2016; Palomo et al., 2015). IL-1 cytokine families are potent activators of classical NF- $\kappa$ B signaling (Vallabhapurapu and Karin, 2009). Activated NF- $\kappa$ B signaling pathway promotes fibroblast differentiation (Tian et al., 2015). IL1R2 may function as an inhibitor of the IL-1/NF- $\kappa$ B pathway to inhibit fibroblast differentiation (Tian et al., 2015). CD69 controls tissue fibrosis by regulating Th17-mediated inflammation (Liappas et al., 2016). CD69 suppresses mTOR signaling (Notario et al., 2018). The abrogation of the mTORC2-Akt signaling axis impeded fibroblast differentiation (Kim et al., 2019). Thus, CD69 may suppress fibroblast differentiation by down-regulating the mTOR signaling pathway. Both of these proteins participate in the MAPK/PI3K/AKT signaling pathway. The transcriptional repressor TGIF2 is critical in TGF $\beta$  signaling to mediate the antifibrotic effect (Melhuish et al., 2016; Sharma et al., 2015). TGF $\beta$  is the most well-known inducer of fibroblast differentiation (Carthy, 2018). It is possible that TGIF2 represses fibroblasts differentiation through negatively regulating the TGF $\beta$  signaling pathway. Within the 50 DEGs that were predicted to have POU2F1

binding sites, some of these genes belong to the reported signaling pathway involved in the mechanosensing of ECM stiffness. In the PubMed database, 27 DEGs were associated with the TGF $\beta$  signaling pathway, 13 DEGs were associated with the ROCK signaling pathway, 4 DEGs were associated with the Hippo signaling pathway, 37 DEGs were associated with the MAPK signaling pathway, and 3 DEGs were associated with the AGE-RAGE signaling pathway (Table S6 in Supporting Information). All of these signaling pathways were reported to participate in stiffness-induced CF differentiation (Herum et al., 2017). These bioinformatics data suggest the core position of POU2F1 in this process.

In conclusion, pathological substrate stiffness promotes the differentiation of CFs into myofibroblasts. The underlying mechanism is that pathological stiffness upregulates expression of POU2F1, resulting in decreased expression of the fibrosis repressor genes IL1R2, CD69 and TGIF2, and consequently contributes to CF differentiation. The present study clarified the role of POU2F1 in pathological substrate stiffness-induced CF differentiation and provided a new target for the treatment of cardiac fibrosis.

## MATERIALS AND METHODS

### Isolation and culture of CFs

All experiments conformed to the US National Institutes of Health Guide for the Care and Use of Laboratory Animals (NIH Publication No. 85-23, revised 2011). Animal experiments were approved by the Committee of Peking University on Ethics of Animal Experiments (LA 2016018) and were conducted in accordance with the ARRIVE (Animal Research: Reporting *In Vivo* Experiments) guidelines and the Guidelines for Animal Experiments, Peking University Health Science Center.

CF cells were isolated and cultured from the hearts of 8- to 10-week-old male C57BL/6 mice as previously described with minor modifications (Takeda et al., 2010). The heart was isolated and digested with 0.1% collagenase type II (300U, 17101-015, Gibco, USA) at 37°C. After centrifugation at 1,000 r min<sup>-1</sup> for 5 min, the supernatant was removed, and the obtained cells were transferred to 10-cm dishes and cultured in DMEM (12800-058, Gibco, USA) supplemented with 10% fetal bovine serum (15140-122, Gibco, USA) in a humidified atmosphere at 37°C and 5% CO<sub>2</sub>. Cells of the second passage were seeded onto substrates with different stiffness for further investigation. CFs were grown on hydrogels for one day and were then subjected to assays.

### Mouse MI model

Ten-week-old male C57BL/6 mice were used in the MI model. The mice were randomly assigned to either the MI

group (surgery to induce MI by occlusion of the left coronary artery) or the sham group (same operation but without left coronary artery occlusion). The surgical procedures were performed after the righting reflex disappeared under anesthesia with 1%–2% isoflurane.

### Preparation of polyacrylamide hydrogels

Polyacrylamide (PA) hydrogels were prepared following the previous protocols (Minisah et al., 2016). Briefly, 25 mm × 25 mm glass microscope slides were treated with NaOH, 3-aminopropyltrimethoxysilane, and glutaraldehyde in a step-by-step manner. After the slides were extensively washed with distilled H<sub>2</sub>O, the slides were ready to support the polyacrylamide gels. Four prepolymer solutions with different acrylamide/bisacrylamide percentage (w/v) ratios were prepared to achieve elastic moduli of 7.5 kPa (10% acrylamide and 0.03% bisacrylamide), 13 kPa (10% acrylamide and 0.07% bisacrylamide), 19.5 kPa (10% acrylamide and 0.13% bisacrylamide), and 35 kPa (10% acrylamide and 0.26% bisacrylamide) and similar porosity. After polymerization, the gel surface was derivatized with the hetero-bifunctional cross-linker Sulfo-SANPAH (Thermo Fisher Scientific, USA) and UV irradiation. Rat-tail collagen (Sigma, USA) was diluted in PBS at 100 µg mL<sup>-1</sup>, spread onto each coverslip and incubated for 18 h at 4°C. The hydrogels on coverslips were rinsed with PBS and sterilized by UV before the cells were seeded. CFs were grown on different gels for one day and then subjected to assays.

### Western blotting

Cell lysates were subjected to sodium dodecyl sulfate-polyacrylamide gel electrophoresis and blotted on nitrocellulose membranes. The membranes were then incubated with antibodies against fibronectin (ab2413, Abcam, USA), αSMA (ab32575, Abcam, USA), POU2F1 (ab178869, Abcam, USA), IL1R2 (sc-376247, Santa Cruz Biotech, USA), CD69 (ab202909, Abcam, USA), TGIF2 (ab190152, Abcam, USA), and GAPDH (2118S, CST). The bands were visualized with SuperSignal West Dura Extended Duration Substrate (Thermo Fisher Scientific, USA). Band intensity was quantitated using NIH ImageJ software (Wu et al., 2019).

### Chromatin immunoprecipitation (ChIP)

Formaldehyde (1%) was used to crosslink proteins and their bound DNA in live CFs. The lysates were then collected and sonicated to shear DNA into fragments of 500–600 bp in length. An antibody against POU2F1 (ab178869, Abcam, USA) and a rabbit IgG antibody were used for immunoprecipitation. The primers used to detect the binding of

POU2F1 to the POU2F1 binding sites in the promoters of mouse IL1R2, CD69, and TGIF2 are listed in Table S7 in Supporting Information.

### Quantitative real-time PCR (qRT-PCR)

Total RNA was extracted from fibroblasts by using TRIzol Reagent (Invitrogen, USA) according to the manufacturer's protocol. cDNA was synthesized in a 20 µL reverse transcription reaction system (M-MLV Reverse Transcription System, Promega Corporation, USA). qRT-PCR was performed on the Mastercycler ep Realplex2 Real-Time PCR System (Eppendorf, Germany) using SYBR Green Mix (TransGen Biotech, Beijing, China). The expression levels of the POU2F1, IL1R2, CD69, and TGIF2 genes were expressed as ratios to that of GAPDH, a housekeeping gene. The sequences of the gene-specific primers are as follows: POU2F1 forward: 5'-GTAAGCTCTGCCTCCTGGTG-3', POU2F1 reverse: 5'-GCTGTCGTTCTCCTGTAGCC-3'; IL1R2 forward: 5'-GAATACACAGCTCCAGGCTCC-3', IL1R2 reverse: 5'-CTGGAGATGTCGGAGTGAGG-3'; CD69 forward: 5'-TGTGTGGAATAGAGCGGAGA-3', CD69 reverse: 5'-AACTAGGTCAAGCCAGGCAA-3'; TGIF2 forward: 5'-TCAAAGATGGTGTCCCTCGC-3', TGIF2 reverse: 5'-ACATCCGGTCCATGGTGAAC-3'; and GAPDH forward: 5'-TCCTGGTATGACAATGAA-TACGGC-3', GAPDH reverse: 5'-TCTTGCTCAGTGTC-CTTGCTGG-3'.

### siRNA transfection of fibroblasts

Fibroblasts were transfected with POU2F1 siRNA (sc-36120, Santa Cruz Biotech, USA) or control siRNA (sc-37007, Santa Cruz Biotech, USA) at 80 nmol L<sup>-1</sup> with Hi-PerFect Transfection Reagent (301705, QIAGEN, USA). Experiments were performed 24 h (for mRNA) or 72 h (for protein) after the cells were transfected.

### Adenovirus expressing POU2F1

Adenovirus expressing POU2F1 (ad-POU2F1) and vector-containing adenovirus (ad-GFP) were purchased from Han-Bio Co., Ltd. (Shanghai, China). The adenoviral vector ad-GFP was used as a control (ad-Ctrl). CFs were infected with ad-POU2F1 or ad-Ctrl followed by the collection of cellular samples.

### Immunofluorescence and imaging

The cells were fixed with 4% paraformaldehyde for 15 min in PBS, permeabilized with 0.2% Triton X-100, blocked with 5% BSA and then stained with primary antibodies against αSMA (ab32575, Abcam, USA), fibronectin (ab2413, Ab-

cam, USA), and POU2F1 (ab178869, Abcam, USA), followed by Alexa Fluor 488 secondary antibodies. The cells were incubated with Hoechst (Invitrogen, USA) for 8 min at room temperature to stain the nuclei. Cells were then incubated with rhodamine phalloidin dye (R415, Invitrogen, USA) for 20 min at room temperature to stain F-actin. For high-content screening imaging, stained cells were visualized and analyzed by a Cellomics ArrayScan VTI HCS Reader (Thermo Fisher Scientific, USA) with the Morphology Explorer BioApplication. For confocal imaging, stained cells were visualized using a laser scanning confocal microscope (LSM780, ZEISS, Germany) with a 20× or 63×/1.4NA oil immersion objective lens and excitation wavelengths of 405 or 488 nm. The images were acquired and analyzed using ZEN 2012 software.

### Bioinformatics

Transcriptomic data were downloaded from NCBI's Gene Expression Omnibus (GEO). We used data from GSE113277 (Yu et al., 2018), RNA-seq data from comparing samples from CFs cultured on 2D 8 kPa (softer) and 64 kPa (stiffer) substrates. Differential expression analysis was performed with the R package edgeR (<https://www.rproject.org>) (Robinson et al., 2010). Cutoff values with a fold-change greater than 2 and a *P* value less than 0.05 were considered significant. Data were log-transformed before analysis. DAVID was used to conduct GO analysis (<https://david.ncifcrf.gov/>). Terms with a *P* value <0.05 were considered. STRING analysis (Szklarczyk et al., 2011) was used to predict protein relationships. The position weight matrix algorithm in TRANSFAC (Wingender et al., 1997) was used to predict potential transcription factors.

### Statistical analysis

All experiments were repeated at least 3 times. The results are expressed as the mean±SD. Statistical analyses were performed using SPSS statistical program or GraphPad Prism 5.0. For parametric data, Student's *t*-test or analysis of variance (ANOVA) combined with Tukey's post hoc test was used to analyze the differences among groups if the data were normally distributed. For data with unequal variances, Welch's *t*-test or ANOVA with Games-Howell post-hoc test was used. For non-parametric data, the Mann-Whitney U-test with the exact method was used to analyze the differences between two groups. The Kruskal-Wallis ANOVA combined with post hoc Dunn's multiple comparison test was performed when more than two groups were evaluated. Differences were considered statistically significant at *P* values <0.05.

**Compliance and ethics** The author(s) declare that they have no conflict

of interest.

**Acknowledgements** The authors acknowledge the support of a grant from the National Natural Science Foundation of China (81530009 to Y.Y.Z.), a grant from the National Natural Science Foundation of China (81822003 and 81670205 to H.X.) and a grant from Natural Science Foundation of Beijing Municipality (7191013 to E.D.D.).

### References

- Allen, D.L., Weber, J.N., Sycuro, L.K., and Leinwand, L.A. (2005). Myocyte enhancer factor-2 and serum response factor binding elements regulate fast myosin heavy chain transcription *in vivo*. *J Biol Chem* 280, 17126–17134.
- Aragona, M., Panciera, T., Manfrin, A., Giullitti, S., Michielin, F., Elvassore, N., Dupont, S., and Piccolo, S. (2013). A mechanical checkpoint controls multicellular growth through YAP/TAZ regulation by actin-processing factors. *Cell* 154, 1047–1059.
- Berry, M.F., Engler, A.J., Woo, Y.J., Pirolli, T.J., Bish, L.T., Jayasankar, V., Morine, K.J., Gardner, T.J., Discher, D.E., and Sweeney, H.L. (2006). Mesenchymal stem cell injection after myocardial infarction improves myocardial compliance. *Am J Physiol Heart Circ Physiol* 290, H2196–H2203.
- Borlak, J., and Thum, T. (2002). PCBs alter gene expression of nuclear transcription factors and other heart-specific genes in cultures of primary cardiomyocytes: possible implications for cardiotoxicity. *Xenobiotica* 32, 1173–1183.
- Borthwick, L.A. (2016). The IL-1 cytokine family and its role in inflammation and fibrosis in the lung. *Semin Immunopathol* 38, 517–534.
- Boulon, S., Dantanel, J.C., Binet, V., Vie, A., Blanchard, J.M., Hipskind, R. A., and Philips, A. (2002). Oct-1 potentiates CREB-driven cyclin D1 promoter activation via a phospho-CREB- and CREB binding protein-independent mechanism. *Mol Cell Biol* 22, 7769–7779.
- Cairns, R.A., Harris, I.S., and Mak, T.W. (2011). Regulation of cancer cell metabolism. *Nat Rev Cancer* 11, 85–95.
- Carthy, J.M. (2018). TGFβ signaling and the control of myofibroblast differentiation: Implications for chronic inflammatory disorders. *J Cell Physiol* 233, 98–106.
- Codelia, V.A., Sun, G., and Irvine, K.D. (2014). Regulation of YAP by mechanical strain through Jnk and Hippo signaling. *Curr Biol* 24, 2012–2017.
- Conrad, C.H., Brooks, W.W., Hayes, J.A., Sen, S., Robinson, K.G., and Bing, O.H.L. (1995). Myocardial fibrosis and stiffness with hypertrophy and heart failure in the spontaneously hypertensive rat. *Circulation* 91, 161–170.
- Driesen, R.B., Nagaraju, C.K., Abi-Char, J., Coenen, T., Lijnen, P.J., Fagard, R.H., Sipido, K.R., and Petrov, V.V. (2014). Reversible and irreversible differentiation of cardiac fibroblasts. *Cardiovasc Res* 101, 411–422.
- Dritsoula, A., Papaioannou, I., Guerra, S.G., Fonseca, C., Martin, J., Herrick, A.L., Abraham, D.J., Denton, C.P., and Ponticos, M. (2018). Molecular basis for dysregulated activation of NKX2-5 in the vascular remodeling of systemic sclerosis. *Arthritis Rheumatol* 70, 920–931.
- Dupont, S., Morsut, L., Aragona, M., Enzo, E., Giullitti, S., Cordenonsi, M., Zanconato, F., Le Digabel, J., Forcato, M., Bicciato, S., et al. (2011). Role of YAP/TAZ in mechanotransduction. *Nature* 474, 179–183.
- Elson, E.L., Qian, H., Fee, J.A., and Wakatsuki, T. (2019). A model for positive feedback control of the transformation of fibroblasts to myofibroblasts. *Prog Biophys Mol Biol* 144, 30–40.
- Engler, A.J., Carag-Krieger, C., Johnson, C.P., Raab, M., Tang, H.Y., Speicher, D.W., Sanger, J.W., Sanger, J.M., and Discher, D.E. (2008). Embryonic cardiomyocytes beat best on a matrix with heart-like elasticity: scar-like rigidity inhibits beating. *J Cell Sci* 121, 3794–3802.
- Engler, A.J., Sen, S., Sweeney, H.L., and Discher, D.E. (2006). Matrix elasticity directs stem cell lineage specification. *Cell* 126, 677–689.

- Feng, Y., Zhang, Y., and Xiao, H. (2018). AMPK and cardiac remodelling. *Sci China Life Sci* 61, 14–23.
- Gyongyosi, M., Winkler, J., Ramos, I., Do, Q.T., Firat, H., McDonald, K., González, A., Thum, T., Díez, J., Jaisser, F., et al. (2017). Myocardial fibrosis: biomedical research from bench to bedside. *Eur J Heart Fail* 19, 177–191.
- Herum, K.M., Choppe, J., Kumar, A., Engler, A.J., and McCulloch, A.D. (2017). Mechanical regulation of cardiac fibroblast profibrotic phenotypes. *Mol Biol Cell* 28, 1871–1882.
- Herum, K.M., Lunde, I.G., McCulloch, A.D., and Christensen, G. (2017). The soft- and hard-heartedness of cardiac fibroblasts: mechanotransduction signaling pathways in fibrosis of the heart. *J Clin Med* 6, 53.
- Hinz, B. (2009). Tissue stiffness, latent TGF- $\beta$  1 Activation, and mechanical signal transduction: Implications for the pathogenesis and treatment of fibrosis. *Curr Rheumatol Rep* 11, 120–126.
- Hinz, B., Phan, S.H., Thannickal, V.J., Galli, A., Bochaton-Piallat, M.L., and Gabbiani, G. (2007). The myofibroblast. *Am J Pathol* 170, 1807–1816.
- Huelsz-Prince, G., Belkin, A.M., VanBavel, E., and Bakker, E.N.T.P. (2013). Activation of extracellular transglutaminase 2 by mechanical force in the arterial wall. *J Vasc Res* 50, 383–395.
- Jenkins, G. (2008). The role of proteases in transforming growth factor- $\beta$  activation. *Int J Biochem Cell Biol* 40, 1068–1078.
- Kang, J., Gemberling, M., Nakamura, M., Whitby, F.G., Handa, H., Fairbrother, W.G., and Tantin, D. (2009). A general mechanism for transcription regulation by Oct1 and Oct4 in response to genotoxic and oxidative stress. *Genes Dev* 23, 208–222.
- Kang, J., Shen, Z., Lim, J.M., Handa, H., Wells, L., and Tantin, D. (2013). Regulation of Oct1/Pou2f1 transcription activity by O-GlcNAcylation. *FASEB J* 27, 2807–2817.
- Kim, S.W., Kim, H.I., Thapa, B., Nuwromenge, S., and Lee, K. (2019). Critical role of mTORC2-Akt signaling in TGF- $\beta$ 1-induced myofibroblast differentiation of human pterygium fibroblasts. *Invest Ophthalmol Vis Sci* 60, 82–92.
- Kong, P., Christia, P., and Frangogiannis, N.G. (2014). The pathogenesis of cardiac fibrosis. *Cell Mol Life Sci* 71, 549–574.
- Lakich, M.M., Diagana, T.T., North, D.L., and Whalen, R.G. (1998). MEF-2 and Oct-1 bind to two homologous promoter sequence elements and participate in the expression of a skeletal muscle-specific gene. *J Biol Chem* 273, 15217–15226.
- Li, L., Zhao, Q., and Kong, W. (2018). Extracellular matrix remodeling and cardiac fibrosis. *Matrix Biol* 68–69, 490–506.
- Li, L., and Chaikof, E.L. (2002). Mechanical stress regulates syndecan-4 expression and redistribution in vascular smooth muscle cells. *Arterioscler Thromb Vasc Biol* 22, 61–68.
- Liappas, G., González-Mateo, G.T., Sánchez-Díaz, R., Lazcano, J.J., Lasarte, S., Matesanz-Marin, A., Zur, R., Ferrantelli, E., Ramirez, L.G., Aguilera, A., et al. (2016). Immune-regulatory molecule CD69 controls peritoneal fibrosis. *J Am Soc Nephrol* 27, 3561–3576.
- Liu, C., Luo, J.W., Liang, T., Lin, L.X., Luo, Z.P., Zhuang, Y.Q., and Sun, Y.L. (2018). Matrix stiffness regulates the differentiation of tendon-derived stem cells through FAK-ERK1/2 activation. *Exp Cell Res* 373, 62–70.
- Maddox, J., Shakya, A., South, S., Shelton, D., Andersen, J.N., Chidester, S., Kang, J., Gligorich, K.M., Jones, D.A., Spangrude, G.J., et al. (2012). Transcription factor Oct1 is a somatic and cancer stem cell determinant. *PLoS Genet* 8, e1003048.
- Magne, S., Caron, S., Charon, M., Rouyez, M.C., and Dusanter-Fourt, I. (2003). STAT5 and Oct-1 form a stable complex that modulates cyclin D1 expression. *Mol Cell Biol* 23, 8934–8945.
- Melhuish, T.A., Taniguchi, K., and Wotton, D. (2016). Tgif1 and Tgif2 regulate axial patterning in mouse. *PLoS ONE* 11, e0155837.
- Minaisah, R.M., Cox, S., and Warren, D.T. (2016). The use of polyacrylamide hydrogels to study the effects of matrix stiffness on nuclear envelope properties. *Methods Mol Biol* 1411, 233–239.
- Ni, J., Dong, Z., Han, W., Kondrikov, D., and Su, Y. (2013). The role of RhoA and cytoskeleton in myofibroblast transformation in hyperoxic lung fibrosis. *Free Radic Biol Med* 61, 26–39.
- Notario, L., Alari-Pahissa, E., Albentosa, A., Leiva, M., Sabio, G., and Lauzurica, P. (2018). Anti-CD69 therapy induces rapid mobilization and high proliferation of HSPCs through S1P and mTOR. *Leukemia* 32, 1445–1457.
- Palomo, J., Dietrich, D., Martin, P., Palmer, G., and Gabay, C. (2015). The interleukin (IL)-1 cytokine family—Balance between agonists and antagonists in inflammatory diseases. *Cytokine* 76, 25–37.
- Pankov, R., and Yamada, K.M. (2002). Fibronectin at a glance. *J Cell Sci* 115, 3861–3863.
- Rahaman, S.O., Grove, L.M., Paruchuri, S., Southern, B.D., Abraham, S., Niese, K.A., Scheraga, R.G., Ghosh, S., Thodeti, C.K., Zhang, D.X., et al. (2014). TRPV4 mediates myofibroblast differentiation and pulmonary fibrosis in mice. *J Clin Invest* 124, 5225–5238.
- Robertson, I.B., Horiguchi, M., Zilberberg, L., Dabovic, B., Hadjiolova, K., and Rifkin, D.B. (2015). Latent TGF- $\beta$ -binding proteins. *Matrix Biol* 47, 44–53.
- Robinson, M.D., McCarthy, D.J., and Smyth, G.K. (2010). edgeR: a bioconductor package for differential expression analysis of digital gene expression data. *Bioinformatics* 26, 139–140.
- Scheibner, K.A., Lutz, M.A., Boodoo, S., Fenton, M.J., Powell, J.D., and Horton, M.R. (2006). Hyaluronan fragments act as an endogenous danger signal by engaging TLR2. *J Immunol* 177, 1272–1281.
- Segura, A.M., Frazier, O.H., and Buja, L.M. (2014). Fibrosis and heart failure. *Heart Fail Rev* 19, 173–185.
- Shakya, A., Kang, J., Chumley, J., Williams, M.A., and Tantin, D. (2011). Oct1 is a switchable, bipotential stabilizer of repressed and inducible transcriptional states. *J Biol Chem* 286, 450–459.
- Sharma, A., Sinha, N.R., Siddiqui, S., and Mohan, R.R. (2015). Role of 5' TG3'-interacting factors (TGIFs) in vorinostat (HDAC inhibitor)-mediated corneal fibrosis inhibition. *Mol Vis* 21, 974–984.
- Shi, X., Qin, L., Zhang, X., He, K., Xiong, C., Fang, J., Fang, X., and Zhang, Y. (2011). Elasticity of cardiac cells on the polymer substrates with different stiffness: an atomic force microscopy study. *Phys Chem Chem Phys* 13, 7540–7545.
- Shimizu, K., Nakajima, A., Sudo, K., Liu, Y., Mizoroki, A., Ikarashi, T., Horai, R., Kakuta, S., Watanabe, T., and Iwakura, Y. (2015). IL-1 receptor type 2 suppresses collagen-induced arthritis by inhibiting IL-1 signal on macrophages. *J Immunol* 194, 3156–3168.
- Song, Y., Zhan, L., Yu, M., Huang, C., Meng, X., Ma, T., Zhang, L., and Li, J. (2014). TRPV4 channel inhibits TGF- $\beta$ 1-induced proliferation of hepatic stellate cells. *PLoS ONE* 9, e101179.
- Souders, C.A., Bowers, S.L.K., and Baudino, T.A. (2009). Cardiac fibroblast. *Circ Res* 105, 1164–1176.
- Strand, M.E., Aronsen, J.M., Braathen, B., Sjaastad, I., Kvaløy, H., Tønnessen, T., Christensen, G., and Lunde, I.G. (2015). Shedding of syndecan-4 promotes immune cell recruitment and mitigates cardiac dysfunction after lipopolysaccharide challenge in mice. *J Mol Cell Cardiol* 88, 133–144.
- Sturm, R.A., Das, G., and Herr, W. (1988). The ubiquitous octamer-binding protein Oct-1 contains a POU domain with a homeo box subdomain. *Genes Dev* 2, 1582–1599.
- Szklarczyk, D., Franceschini, A., Kuhn, M., Simonovic, M., Roth, A., Minguez, P., Doerks, T., Stark, M., Muller, J., Bork, P., et al. (2011). The STRING database in 2011: functional interaction networks of proteins, globally integrated and scored. *Nucleic Acids Res* 39, D561–D568.
- Takeda, N., Manabe, I., Uchino, Y., Eguchi, K., Matsumoto, S., Nishimura, S., Shindo, T., Sano, M., Otsu, K., Snider, P., et al. (2010). Cardiac fibroblasts are essential for the adaptive response of the murine heart to pressure overload. *J Clin Invest* 120, 254–265.
- Talman, V., and Ruskoaho, H. (2016). Cardiac fibrosis in myocardial infarction—from repair and remodeling to regeneration. *Cell Tissue Res* 365, 563–581.
- Taylor, K.R., Trowbridge, J.M., Rudisill, J.A., Termeer, C.C., Simon, J.C., and Gallo, R.L. (2004). Hyaluronan fragments stimulate endothelial



- recognition of injury through TLR4. *J Biol Chem* 279, 17079–17084.
- Thomas, K.S., Owen, K.A., Conger, K., Llewellyn, R.A., Bouton, A.H., and Casanova, J.E. (2019). Non-redundant functions of FAK and Pyk2 in intestinal epithelial repair. *Sci Rep* 9, 4497.
- Tian, J., Avalos, A.M., Mao, S.Y., Chen, B., Senthil, K., Wu, H., Parroche, P., Drabic, S., Golenbock, D., Sirois, C., et al. (2007). Toll-like receptor 9-dependent activation by DNA-containing immune complexes is mediated by HMGB1 and RAGE. *Nat Immunol* 8, 487–496.
- Tian, K., Liu, Z., Wang, J., Xu, S., You, T., and Liu, P. (2015). Sirtuin-6 inhibits cardiac fibroblasts differentiation into myofibroblasts via inactivation of nuclear factor  $\kappa$ B signaling. *Transl Res* 165, 374–386.
- Torres, W.M., Jacobs, J., Doviak, H., Barlow, S.C., Zile, M.R., Shazly, T., and Spinale, F.G. (2018). Regional and temporal changes in left ventricular strain and stiffness in a porcine model of myocardial infarction. *Am J Physiol Heart Circ Physiol* 315, H958–H967.
- Turner, N.A. (2014). Effects of interleukin-1 on cardiac fibroblast function: relevance to post-myocardial infarction remodelling. *Vasc Pharmacol* 60, 1–7.
- Vabulas, R.M., Ahmad-Nejad, P., da Costa, C., Miethke, T., Kirschning, C. J., Häcker, H., and Wagner, H. (2001). Endocytosed HSP60s use toll-like receptor 2 (TLR2) and TLR4 to activate the toll/interleukin-1 receptor signaling pathway in innate immune cells. *J Biol Chem* 276, 31332–31339.
- Vallabhapurapu, S., and Karin, M. (2009). Regulation and function of NF- $\kappa$ B transcription factors in the immune system. *Annu Rev Immunol* 27, 693–733.
- van Putten, S., Shafieyan, Y., and Hinz, B. (2016). Mechanical control of cardiac myofibroblasts. *J Mol Cell Cardiol* 93, 133–142.
- Vazquez-Arreaguin, K., and Tantin, D. (2016). The Oct1 transcription factor and epithelial malignancies: old protein learns new tricks. *Biochim Biophys Acta Gene Regul Mech* 1859, 792–804.
- Wang, N., Tytell, J.D., and Ingber, D.E. (2009). Mechanotransduction at a distance: mechanically coupling the extracellular matrix with the nucleus. *Nat Rev Mol Cell Biol* 10, 75–82.
- Wingender, E., Karas, H., and Knuppel, R. (1997). TRANSFAC database as a bridge between sequence data libraries and biological function. In Proceedings of the 2nd Pacific Symposium on Biocomputing (Maui, HI, USA), pp. 477–485.
- Wu, J., Deng, X., Gao, J., Gao, W., Xiao, H., Wang, X., and Zhang, Y. (2019). Autophagy mediates the secretion of macrophage migration inhibitory factor from cardiomyocytes upon serum-starvation. *Sci China Life Sci* 62, 1038–1046.
- Wu, Y., Cazorla, O., Labeit, D., Labeit, S., and Granzier, H. (2000). Changes in titin and collagen underlie diastolic stiffness diversity of cardiac muscle. *J Mol Cell Cardiol* 32, 2151–2161.
- Xie, J., Zhang, Q., Zhu, T., Zhang, Y., Liu, B., Xu, J., and Zhao, H. (2014). Substrate stiffness-regulated matrix metalloproteinase output in myocardial cells and cardiac fibroblasts: implications for myocardial fibrosis. *Acta Biomater* 10, 2463–2472.
- Yang, J., Savvatis, K., Kang, J.S., Fan, P., Zhong, H., Schwartz, K., Barry, V., Mikels-Vigdal, A., Karpinski, S., Korniyev, D., et al. (2016). Targeting LOXL2 for cardiac interstitial fibrosis and heart failure treatment. *Nat Commun* 7, 13710.
- Yu, J., Seldin, M.M., Fu, K., Li, S., Lam, L., Wang, P., Wang, Y., Huang, D., Nguyen, T.L., Wei, B., et al. (2018). Topological arrangement of cardiac fibroblasts regulates cellular plasticity. *Circ Res* 123, 73–85.
- Zaidel-Bar, R., Itzkovitz, S., Ma'ayan, A., Iyengar, R., and Geiger, B. (2007). Functional atlas of the integrin adhesome. *Nat Cell Biol* 9, 858–867.
- Zhang, Y., Ng, H.H., Erdjument-Bromage, H., Tempst, P., Bird, A., and Reinberg, D. (1999). Analysis of the NuRD subunits reveals a histone deacetylase core complex and a connection with DNA methylation. *Genes Dev* 13, 1924–1935.
- Zhao, H., Li, X., Zhao, S., Zeng, Y., Zhao, L., Ding, H., Sun, W., and Du, Y. (2014). Microengineered *in vitro* model of cardiac fibrosis through modulating myofibroblast mechanotransduction. *Biofabrication* 6, 045009.
- Zhou, J., Yi, Q., and Tang, L. (2019). The roles of nuclear focal adhesion kinase (FAK) on cancer: a focused review. *J Exp Clin Cancer Res* 38, 250.
- Zilberberg, L., Todorovic, V., Dabovic, B., Horiguchi, M., Couroussé, T., Sakai, L.Y., and Rifkin, D.B. (2012). Specificity of latent TGF- $\beta$  binding protein (LTBP) incorporation into matrix: Role of fibrillins and fibronectin. *J Cell Physiol* 227, 3828–3836.

## SUPPORTING INFORMATION

The supporting information is available online at <https://doi.org/10.1007/s11427-019-1747-y>. The supporting materials are published as submitted, without typesetting or editing. The responsibility for scientific accuracy and content remains entirely with the authors.